AGU PUBLICATIONS

Geophysical Research Letters

RESEARCH LETTER
10.1002/2017GL072879

Key Points:
- Dynamical systems metrics can identify sets of large-scale atmospheric flow patterns with similar spatial structure and temporal evolution
- These patterns can be interpreted as states of maximum predictability
- These patterns provide predictability of large-scale wintertime surface temperature extremes in Europe up to 1 week in advance

Supporting Information:
- Supporting Information S1

Correspondence to:
G. Messori,
gabriele.messori@misu.su.se

Citation:
Messori, G., R. Caballero, and D. Faranda (2017), A dynamical systems approach to studying midlatitude weather extremes, *Geophys. Res. Lett.*, *44*, doi:10.1002/2017GL072879.

Received 31 JAN 2017
Accepted 27 MAR 2017
Accepted article online 29 MAR 2017

A dynamical systems approach to studying midlatitude weather extremes

Gabriele Messori[1], Rodrigo Caballero[1], and Davide Faranda[2]

[1]Department of Meteorology and Bolin Centre for Climate Research, Stockholm University, Stockholm, Sweden, [2]Laboratoire des Sciences du Climat et de l'Environnement, LSCE/IPSL, CEA-CNRS-UVSQ, Université Paris-Saclay, Gif-sur-Yvette, France

Abstract Extreme weather occurrences carry enormous social and economic costs and routinely garner widespread scientific and media coverage. The ability to predict these events is therefore a topic of crucial importance. Here we propose a novel predictability pathway for extreme events, by building upon recent advances in dynamical systems theory. We show that simple dynamical systems metrics can be used to identify sets of large-scale atmospheric flow patterns with similar spatial structure and temporal evolution on time scales of several days to a week. In regions where these patterns favor extreme weather, they afford a particularly good predictability of the extremes. We specifically test this technique on the atmospheric circulation in the North Atlantic region, where it provides predictability of large-scale wintertime surface temperature extremes in Europe up to 1 week in advance.

Plain Language Summary Extreme weather occurrences carry enormous social and economic costs and routinely garner widespread scientific and media coverage. The ability to predict these events is therefore a topic of crucial importance. Here we propose a novel analysis technique for improving the prediction of extreme events, which identifies the large-scale atmospheric circulation configurations affording the best predictability. We specifically test our technique on the atmospheric circulation in the North Atlantic region, where it provides predictability of large-scale wintertime surface temperature extremes in Europe up to 1 week in advance.

1. Introduction

Dynamical systems techniques provide a rigorous mathematical framework for describing atmospheric flows and, more generally, the climate system. Each instantaneous atmospheric state corresponds to a point in phase space, and the evolution of the atmosphere can thus be described by the trajectory joining these points. Early efforts in this direction showed that atmospheric motions are chaotic and settle on a finite-dimensional attractor—namely, "the collection of all states that the system can assume or approach again and again, as opposed to those that it will ultimately avoid" [*Lorenz*, 1980]. The attractor's average dimension (D) indicates the minimum number of degrees of freedom needed to span the subspace occupied by the attractor. However, two major obstacles have limited the application of dynamical systems analyses to atmospheric motions. First, computing D for systems with a large number of degrees of freedom is nontrivial, and traditional approaches have proved unreliable when applied to atmospheric flows [*Grassberger*, 1986; *Lorenz*, 1991]. Moreover, this approach is ill suited to study extreme weather events, which carry major social and economic costs [e.g., *Kunkel et al.*, 1999; *Gasparrini et al.*, 2015] and attract intense scientific and popular attention [e.g., *Herring et al.*, 2015]. The extremes are associated with transient states of the atmosphere [*Vautard and Ghil*, 1989]. Their study therefore requires instantaneous, local properties, rather than average quantities such as D. Local properties can further provide insights into the stability of the associated atmospheric configuration [*Vannitsem*, 2001].

Here we compute two instantaneous dynamical systems metrics for the atmospheric circulation over the North Atlantic: the instantaneous dimension (d) and the inverse of the persistence time (θ) of the daily mean 500 hPa geopotential height. The local properties of a dynamical system can be fully described by these two quantities [*Lucarini et al.*, 2016]. We then show that they provide a novel pathway for the prediction of extreme weather events. We focus on a societally relevant case: wintertime (December, January, and February—DJF) temperature extremes over Europe. Cold extremes can cause significant increases in mortality [e.g., *Analitis et al.*, 2008], while warm extremes can affect snow and

water availability and crop yields and therefore impact the local economies [e.g., *Gooding et al.*, 2003; *Beniston*, 2005].

The North Atlantic region has been widely studied, and its wintertime dynamics are dominated by well-known large-scale modes of variability, chief among them the North Atlantic Oscillation (NAO). The latter is a key source of atmospheric predictability in the region, across a broad range of time scales [e.g., *Johansson*, 2007; *Ferranti et al.*, 2015]. A method selecting atmospheric configurations offering the maximum predictability would therefore be expected to capture some aspects of this mode while hopefully also offering additional insights. This motivates our choice of the Euro-Atlantic region as the ideal test bed to verify whether our novel methodology is robust while at the same time providing a useful complement to more traditional analyses. However, we stress that our approach is entirely general and may be extended to other variables, seasons, and geographical domains. We further envisage that the metrics we adopt may in the future be applied in an operational forecasting context.

2. Data and Dynamical Systems Metrics

We use daily mean 500 hPa geopotential height and 2 m temperature data from the European Centre for Medium-Range Weather Forecasts' ERA-Interim reanalysis [*Dee et al.*, 2011]. The data sets have a horizontal resolution of 0.75° and 1°, respectively. We focus on the winter seasons (December–February, DJF) during 1979–2011 and select a domain covering the North Atlantic and Europe (75°W–50°E, 25°N–75°N). Previous analyses have shown that the dynamical systems metrics are insensitive to resolution and linearly insensitive to the exact geographical boundaries chosen [*Faranda et al.*, 2017]. Mid-tropospheric geopotential height is extensively used to describe the major modes of variability affecting the North Atlantic [e.g., *Baldwin and Dunkerton*, 2001] and more generally large-scale atmospheric features, including teleconnection patterns, atmospheric blocking, and weather regimes [e.g., *Michelangeli et al.*, 1995; *Davini et al.*, 2012]. We therefore select it as a good proxy for the large-scale atmospheric circulation over the North Atlantic sector.

In order to compute the instantaneous dimension and inverse persistence, we interpret the geopotential height field as a point along the system's trajectory in phase space. The values of d and θ for a specific point in phase space describe the local behavior of the segments of the trajectory that pass close to that point. A scatterplot of d versus θ is shown in Figure S1 in the supporting information. A derivation of the two metrics, based upon *Süveges* [2007], *Freitas et al.* [2010], *Faranda et al.* [2011, 2016], and *Lucarini et al.* [2012, 2016], is provided in the supporting information. d is closely linked to the density of the trajectories (and hence to the local Lyapunov exponents) and provides a measure of the maximum divergence of the trajectories. In simple terms, a given atmospheric state with a low d is more likely to evolve in a similar way to all its neighboring states than a case with high d. θ is the inverse of the average persistence time of trajectories around a given point, and it takes values in [0, 1] [*Leadbetter et al.*, 1983]. Atmospheric states with a low θ are persistent and will therefore evolve—and diverge from neighboring states—slowly. Both quantities are therefore closely linked to the predictability afforded by a given atmospheric state. Figure 1a provides an idealized illustration of the above for trajectories with low instantaneous dimension (blue trajectories) and high persistence (red trajectories).

We focus here on atmospheric configurations which have both low d and low θ, namely, the states that should provide the maximum predictability of the trajectories' forward paths. Specifically, we consider days where both d and θ are in the lowest 20 percentiles of their respective distributions. For the case of several consecutive days satisfying this condition, we select the first day in the series. The rationale behind this choice is to extract the maximum forward predictability from the metrics. This is also the most practical option for use in operational contexts. Say, for example, that we opted to select the local minimum of each threshold exceedance rather than the first day. For a series of several days continuously exceeding the threshold, the local minimum could only be determined at the end of the series, while the initial exceedance can be spotted on the day it occurs. We do not simply select all days below the chosen percentile threshold because we wish to avoid double counting when computing lagged composites. We term the selected events *dynamical extremes*. These account for ~4.4% of the time steps, or roughly 4 days every winter. The choice of the 20th percentile as threshold is a compromise between the competing demands of selecting states that can be qualified as dynamical extremes and having a sufficiently large number of events. In fact, our aim is to identify a pathway for predictability which could be applied in an operational forecasting

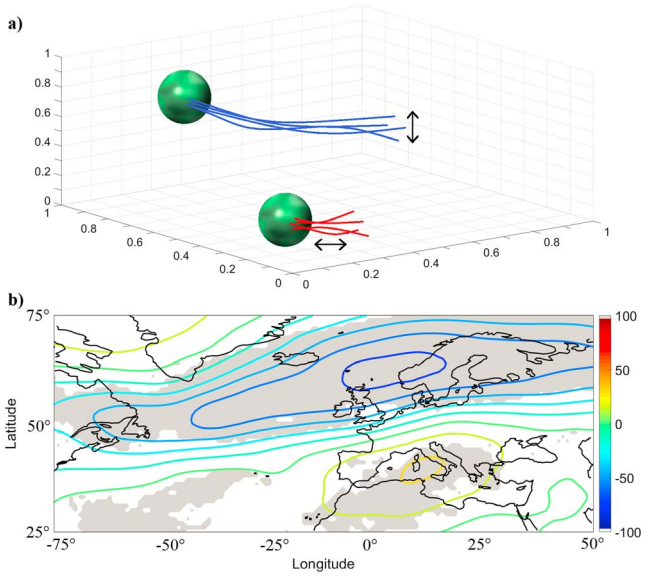

Figure 1. (a) Example of trajectories evolving from neighborhoods (marked by the green spheres) with low instantaneous dimension (blue trajectories) and high persistence (red trajectories) in an idealized three-dimensional phase space. The low dimension implies that the maximum divergence of the blue trajectories is small but gives no information on how rapidly they leave the neighborhood. The high persistence implies that the trajectories are slow in leaving the neighborhood but gives no information on their maximum divergence. (b) Composite 500 hPa geopotential height anomalies (m) for days corresponding to low d and θ. The grey contours mark regions where more than 60% of the members of the composite agree on the sign of the anomalies (see section 2).

context. A result which, for example, were only to apply to 1 day every winter would have a limited value. Reasonable variations in this threshold were tested (22.5th, 17.5th, 12.5th percentiles) and were found not to qualitatively alter our conclusions (not shown).

The 2 m temperature extremes at each grid point are defined as all days exceeding the 10th and 90th percentiles of the local distribution of deseasonalized anomalies. These are standard thresholds used in the literature [e.g., *Yiou and Nogaj*, 2004]; repeating the analysis with the 5th and 95th percentiles (not shown) yields qualitatively similar results. The anomalies are defined as departures from the long-term daily average. For example, the climatological value for the 1 December is given by the mean of all 1 December in the data set. We do not apply the same procedure as for the dynamical extremes to select temperature extremes because these are chosen based on their societal and economic impact rather than on considerations based on atmospheric configurations. It would indeed make little sense to only consider the first in a series of very cold or very warm winter days.

Statistical significance is assessed using both Monte Carlo random sampling with 1000 iterations and a sign test. The former is used to test that the positive (negative) deviations from the climatology associated with the dynamical extremes are significantly more positive (negative) than what would be expected for a random collection of winter days. First, distributions of outcomes based on random sets of winter days with the same number of members as the number of dynamical extremes are created. Next, one-sided 5% significance bounds are obtained directly from the percentiles of these distributions. The sign test is based on sign agreement between the individual members of the composite maps. The fraction of members displaying the same sign as the overall composite is counted at each grid point, and areas where at least 60% of the composited events agree on the sign are identified. Assuming a binomial process with the same number of draws as the dynamical extremes and equal chances of positive or negative outcomes, a 60% threshold is beyond the 99th percentile of the distribution.

3. A Dynamical Systems Predictability Pathway

We now analyze the dynamical extremes as defined in section 2 above. Figure 1b shows the composite 500 hPa geopotential height anomaly patterns for the selected events. These correspond to an anomaly dipole which is reminiscent of a positive NAO phase, albeit shifted to the east. In principle, two points with similar d and θ could represent very different flow configurations. We find that this not be the case: the vast majority of the composite members agree on the sign of the anomalies suggesting that, at least for dynamical extremes, similar flow configurations generally correspond to similar regions in d-θ space. Coherent large-scale features are retained at positive lags, up to ~6–7 days following the selected extremes (Figures S2a, S2c, S2e, and S2g), beyond which sign agreement is largely lost. Consistently with our interpretation of d and θ,

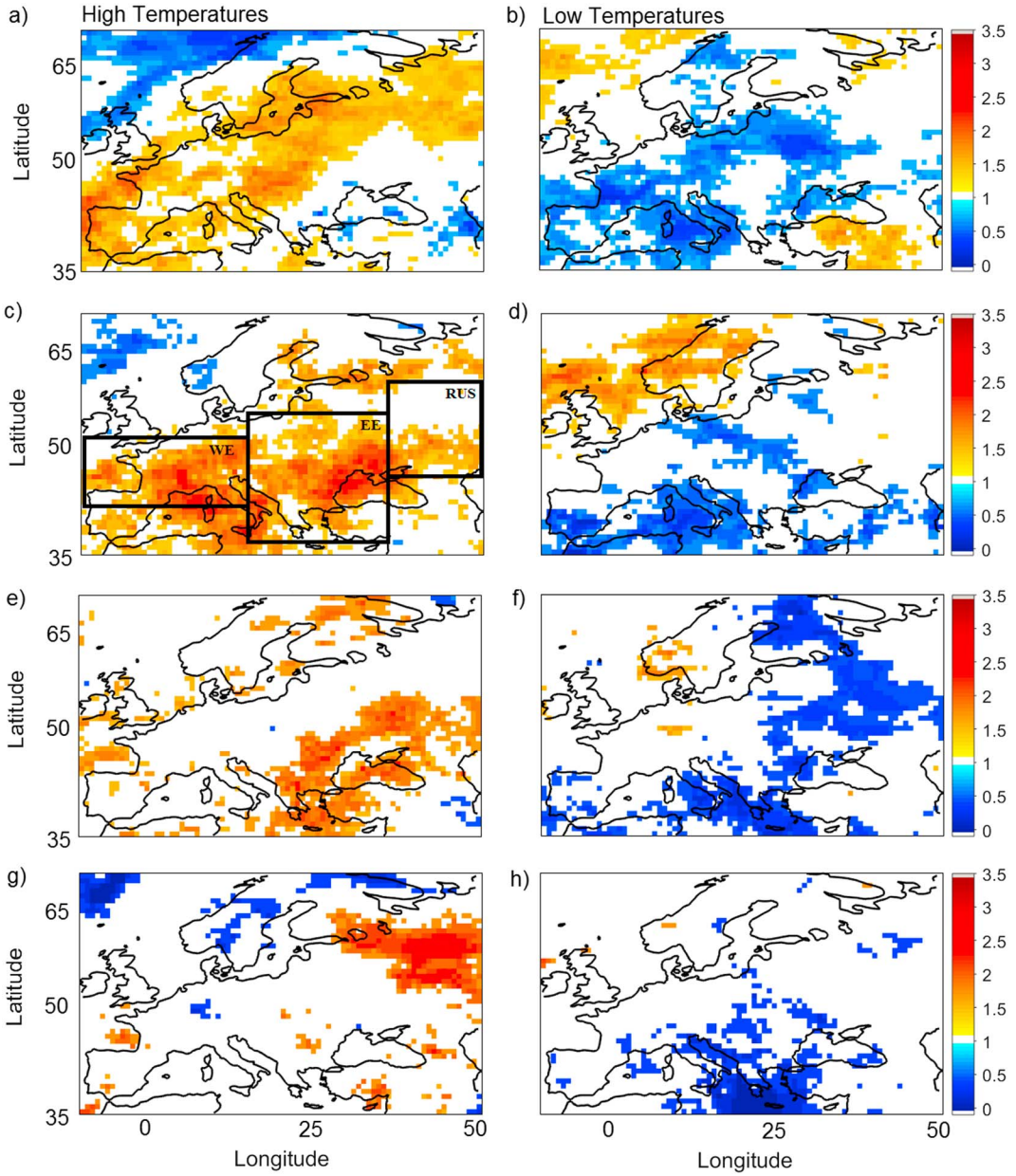

Figure 2. Fractional changes in the frequency of wintertime (a, c, e, and g) hot and (b, d, f, and h) cold surface temperature extremes conditional on low instantaneous dimension and high persistence events relative to the climatology, at lag 0 (Figures 2a and 2b), lag +4 (Figures 2c and 2d), lag +6 (Figures 2e and 2f), and lag +8 days (Figures 2g and 2h). The black boxes in Figure 2c mark the domains used in Figure 4 (see also Table S1). Only statistically significant values obtained from a random sampling procedure are shown (see section 2).

the atmospheric patterns associated with the largest instantaneous dimension and lowest persistence diverge quickly at positive lags, and the geopotential height anomaly composites largely lose coherence by lag +3 (Figures S2b, S2d, S2f, and S2h).

Climate or weather extremes are, by their very definition, rare. They should therefore generally be associated with similarly unusual large-scale atmospheric flow patterns [e.g., *Grotjahn et al.*, 2016]. While there is no guarantee that dynamical extremes correspond to weather extremes at a specific location, it is therefore plausible to expect some correspondence between the two, at least at a continental scale. Figure 2 displays the changes in the frequency of 2 m temperature extremes associated with dynamical extremes, relative to

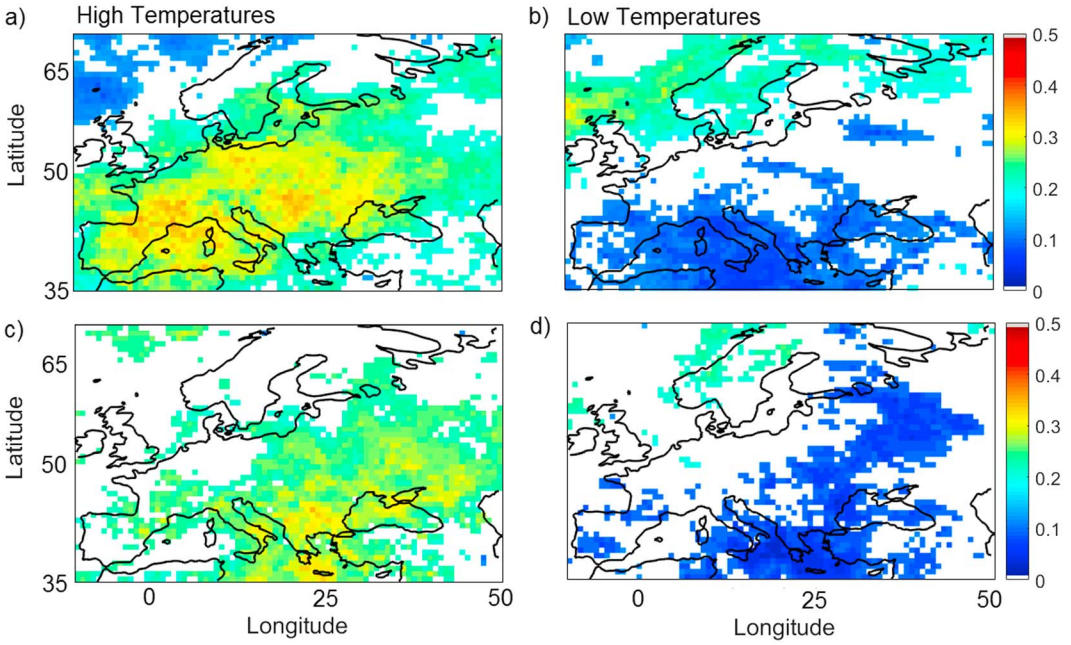

Figure 3. Fraction of low instantaneous dimension and high persistence extremes associated with (a, c) hot and (b, d) cold wintertime surface temperature extremes at a given location, at lags +2 to +4 (Figures 3a and 3b) and lags +5 to +7 days (Figures 3c and 3d). Only statistically significant values obtained from a random sampling procedure are shown (see section 2).

the wintertime climatology. A value of 1 means that the frequency of temperature extremes is insensitive to the dynamical extremes; a value of 0 means that there are no temperature extremes for the selected dynamical extremes; a value of 2 means that there are twice as many temperature extremes as in the climatology. At lag 0 (Figures 2a and 2b) the dynamical extremes correspond to a higher frequency of warm extremes and a decreased frequency of cold extremes across large parts of western, continental and northern Europe. At lag +4 days (Figures 2c and 2d) the pattern is similar but now displays larger-frequency changes for the warm extremes over the Mediterranean. The only regions showing an inverse pattern, with decreased warm occurrences and increased cold occurrences are northern and western Scandinavia and the North Sea. By lag +6 days (Figures 2e and 2f) the largest changes in the temperature extremes have shifted eastward and are now centered over eastern and southeastern Europe. By day +8 (Figures 2g and 2h) there are two main regions of significant changes, with a heightened frequency of warm extremes over western Russia and a decrease in cold extremes over the Eastern Mediterranean. These changes in extreme event frequency are largely consistent with the anomaly patterns shown in Figures 1b and S2. The cyclone-anticyclone dipole associated with the dynamical extremes, which displays a southwest to northeast tilt, draws warm subtropical air over most of Europe, with the exception of northern and western Scandinavia.

We next test the correspondence between dynamical extremes and the individual weather extremes at positive lags. Figure 3 displays the fraction of dynamical extremes which are followed within 2–4 days (Figures 3a and 3b) and 5–7 days (Figures 3c and 3d) by a temperature extreme. Note that if more than one temperature extreme falls within the lag interval for a single dynamical extreme, only one is counted. The dynamical extremes display significant hit rates for both warm and cold extremes across the whole continent up to 7 days. Hit rates for warm extremes locally exceed 40%, while hit rates for cold extremes reach below 4%. In other words, conditioning on a dynamical extreme significantly raises the chances of warm extremes and at the same time essentially excludes the possibility of cold extremes at a regional scale over several days. As expected, there is a good agreement between Figures 2 and 3, with the regions which show the largest positive changes in Figure 2, displaying high-fractional matches in Figure 3.

To further illuminate the predictability afforded by the dynamical extremes, we examine how the lagged distributions of regional temperature anomalies are modulated by the dynamical extremes. We focus on three broad domains selected to cover most of the European continent, marked by the black boxes in Figure 2c

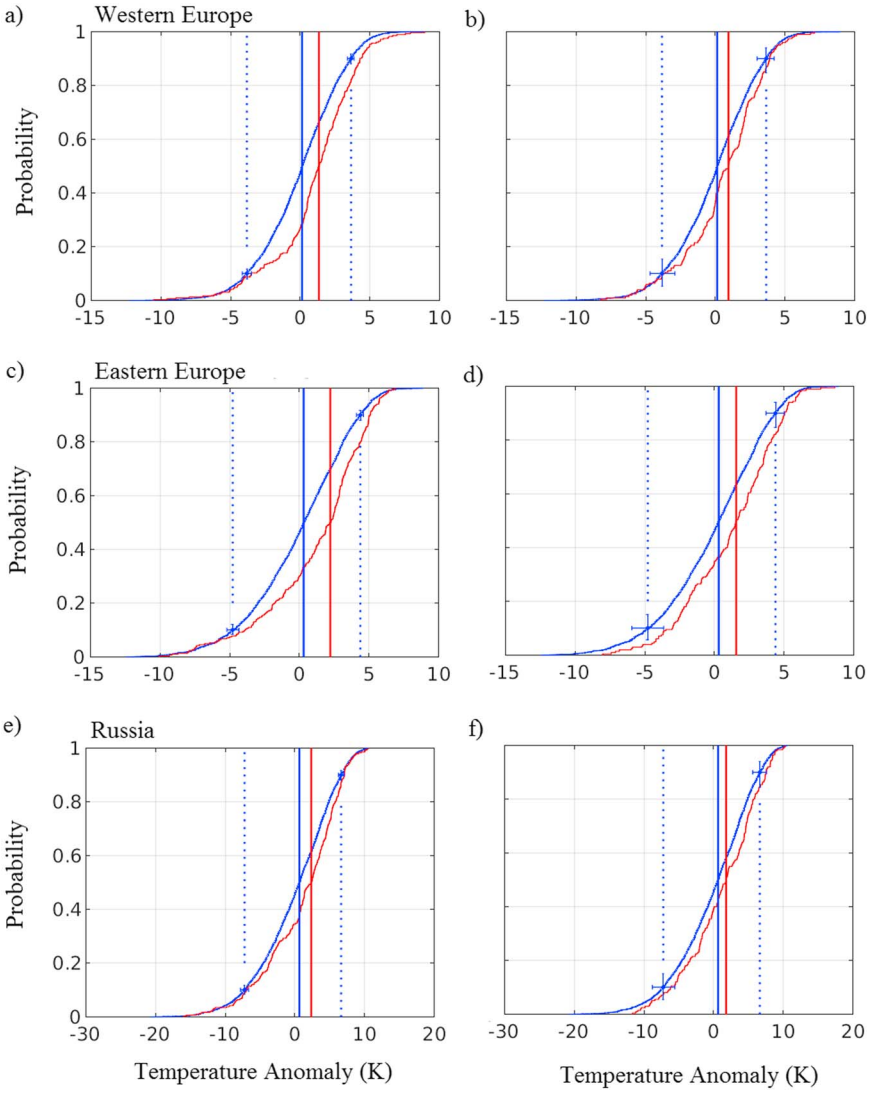

Figure 4. Empirical cumulative distributions of land-only area-averaged 2 m temperature anomalies (K). The blue curves correspond to the wintertime climatology; the red are conditional on the occurrence of a dynamical extreme (a, c, and e) 2 to 4 days and (b, d, and f) 5 to 7 days before. The dashed vertical lines mark the climatological 10th and 90th percentiles. The continuous vertical lines mark the medians of the two distributions. The blue crosses mark the statistical significance for the shift in the percentiles (horizontal bars) and the change in the number of events above/below the climatological percentiles (vertical bars). The edges of the bars correspond to the 5th and 95th percentiles of these quantities computed using a random sampling procedure (see section 2). See Table S1 for the domain boundaries.

(see also Table S1). Figure 4 displays the cumulative distributions of land-only area-averaged temperature anomalies over these domains for the full wintertime climatology (blue) and conditional on the occurrence of a low d and θ episode (red), at lags of -2 to -4 days (Figures 4a, 4c, and 4d) and -5 to -7 days (Figures 4b, 4d, and 4f). In all domains, the dynamical extremes have major effects on the large-scale temperature anomalies. In western Europe they correspond to significant increases in the 90th percentile, and associated changes in the amount of days exceeding them, at short positive lags (Figure 4a). Over Eastern Europe a significant shift in both the 10th and 90th percentiles is seen at both lag ranges (Figures 4c and 4d). Over Russia there is relatively little change in these percentiles at short lags, while at days +5 to +7 there is a marked shift in the 90th percentile of the distribution (Figure 4f). At the same time we note that the shift in the median over this domain is larger for shorter lead times. Finally, we note that all medians of the distributions for dynamical extremes are larger than their climatological counterparts and statistically

different under a Wilcoxon rank sum test [*Mann and Whitney*, 1947] at the 1% significance level. This is fully consistent with the reduction in cold extremes and increase in warm extremes shown in Figure 2.

4. Relation With the NAO

Temperatures extremes over Europe are often discussed in the context of the NAO [e.g., *Yiou and Nogaj*, 2004; *Cassou*, 2008]. The two phases of the NAO are also the initialization states that afford the best predictability in ensemble forecasts [*Ferranti et al.*, 2015]. Since the dynamical extremes should capture the atmospheric configurations offering the best predictability, it is not surprising that they resemble an NAO dipole. At the same time, it is important to highlight that these metrics provide complementary information to an NAO-based analysis. We define a daily NAO index (NAOI) as the difference in average area-weighted 500 hPa height anomalies over the domains (70°W–10°W, 35°N–45°N) and (70°W–10°W, 55°N–70°N). This follows the definition adopted by the National Oceanic and Atmospheric Administration's Physical Sciences Division of the Earth System Research Laboratory (http://www.esrl.noaa.gov/psd/data/timeseries/daily/NAO/). The mean NAOI value for the dynamical extremes is −0.10 at lag −4, 0.22 at lag 0 and 0.15 at lag +4 days. One can further repeat the analysis presented in Figures 2 and 3 selecting NAO+ extremes with the same procedure used for dynamical extremes. We now use the 80th percentile as threshold, so as to obtain a similar number of events to the dynamical extremes (~4.1% instead of ~4.4%). Only ~5.1% of the selected NAO+ extremes match a dynamical extreme; similarly, roughly 25% of days above the NAO+ threshold match days below the dynamical extremes threshold. Consistently with this, the changes in the occurrence of temperature extremes associated with the NAO display some important differences from those seen for the dynamical extremes (cf. Figures 2 and S3). We further note that while at lags 0 and 4 the NAO has a stronger impact on the temperature extremes than the dynamical extremes, the two become comparable around lag +6 and by lag +8 the dynamical extremes display a stronger regional footprint. This is consistent with our interpretation of dynamical extremes as the atmospheric states which give the best forward predictability as opposed to states which instantaneously correspond to the largest temperature anomalies.

5. Discussion and Conclusions

Using simple instantaneous dynamical systems metrics, we identify the most stable and recurrent atmospheric states, which are also the states providing the best forward predictability. We apply this technique to the North Atlantic sector. A large part of the atmospheric variability, and predictability, in this region is associated with the NAO. It is therefore reassuring that the atmospheric configuration we obtain from our dynamical system analysis resembles an NAO dipole. At the same time the high-predictability days we select, termed dynamical extremes, do not systematically match NAO extremes. We therefore conclude that a dynamical systems approach provides complementary information to an NAO-based analysis.

Our results are also in good agreement with a previous analysis by *Vannitsem* [2001]. The author studied the local stability properties of the flow in a quasi-geostrophic model and used them in combination with a clustering algorithm to define regimes affording high and low medium-range predictability. The analysis was performed on a global scale and on an idealized model; we nonetheless note that one of the high-predictability clusters thus identified bears some resemblance in the Atlantic sector with the dipole pattern we associate here with high predictability (cf. our Figure 1b with cluster CL_3 in Vannitsem's Figure 11).

Our dynamical systems perspective further provides a definition of *extreme event* which differs from the standard statistical view formalized by Pickands and Pareto [*Pickands*, 1975], where extremes are large or small events with respect to a certain local observable. For complex fields, the dynamical systems approach can capture the crucial link between large-scale nonstatic phenomena and local effects. In the context of this study, a more traditional definition of a "geopotential extreme" could be, for example, to compute a Euclidean distance of daily fields from the long-term mean field and define extremes as days in the top and bottom percentiles of this distribution. However, if this approach is used, selecting a similar number of occurrences as for the dynamical extremes, the link between the geopotential extremes and the predictability of temperature extremes over Europe is weak (see Figure S4 and Text S2).

On the contrary, the dynamical extremes provide a strong predictability pathway for wintertime temperature extremes over the European continent at time scales of up to a week. This is underscored by the significant modulation of regional temperature extremes associated with dynamical extremes. In this respect, we

highlight that a forecast of a decreased probability of an extreme can be as valuable societally and economically as the forecast of an increased probability of an extreme. The link between dynamical extremes and cold spells is therefore important, even though the extremes systematically correspond to decreased occurrences of low temperatures. An additional analysis considering states with low d and low θ separately (not shown) highlights that, in general, persistence provides a better indication of predictability than instantaneous dimension. This suggests that the rapidity with which nearby trajectories diverge from a neighborhood is typically, but not always, more relevant than their maximum spread while doing so. The insights provided by the two dynamical systems metrics can complement the information issued by deterministic and ensemble forecasts, which are currently used by many national emergency response services [e.g., *Sene*, 2008]. The same metrics could be further used as diagnostic tools to assess the flow-dependent skill of current operational ensemble forecast products. Finally, future forecast systems could use the values of d and θ to determine the optimal resolution and ensemble size for a given initialization step.

The analysis presented in this study points to several pathways for future research. Keeping the focus on the North Atlantic, it is necessary to verify whether the low d and θ states which do not agree with the sign of the geopotential height anomaly composite actually correspond to a separate cluster in phase space relative to the ones that do. This would allow for a more accurate quantification of the predictability afforded by the dynamical extremes. More generally, the methodology we adopt could be applied to domains which, unlike the North Atlantic, might not have a clearly recognizable dominant mode of atmospheric variability. An obvious caveat is that there is no guarantee that dynamical extremes will be associated with a given class of weather extremes over a specific geographical domain, meaning that this technique might not always be appropriate for targeted regional studies. At the same time, we note that the dynamical systems metrics provide a general information about atmospheric trajectories, meaning that their use can be extended to predictability problems unrelated to extreme events. On the more technical side, it will be necessary to provide a robust quantification of the typical predictability horizon afforded by the dynamical systems perspective, by performing a comprehensive analysis on the variability of d and θ and their covariance.

Acknowledgments
During this work, G. Messori has been funded by a grant of the Department of Meteorology of Stockholm University. ERA-Interim reanalysis data are freely available from the ECMWF at http://apps.ecmwf.int/datasets/.

References

Analitis, A., et al. (2008), Effects of cold weather on mortality: Results from 15 European cities within the PHEWE project, *Am. J. Epidemiol.*, *168*(12), 1397–1408.

Baldwin, M. P., and T. J. Dunkerton (2001), Stratospheric harbingers of anomalous weather regimes, *Science*, *294*(5542), 581–584.

Beniston, M. (2005), Warm winter spells in the Swiss alps: Strong heat waves in a cold season? A study focusing on climate observations at the Saentis high mountain site, *Geophys. Res. Lett.*, *32*, L01812, doi:10.1029/2004GL021478.

Cassou, C. (2008), Intraseasonal interaction between the Madden–Julian oscillation and the North Atlantic oscillation, *Nature*, *455*(7212), 523–527.

Davini, P., C. Cagnazzo, S. Gualdi, and A. Navarra (2012), Bidimensional diagnostics, variability, and trends of Northern Hemisphere blocking, *J. Clim.*, *25*(19), 6496–6509.

Dee, D. P., et al. (2011), The ERA-Interim reanalysis: Configuration and performance of the data assimilation system, *Q. J. R. Meteorol. Soc.*, *137*(656), 553–597.

Faranda, D., V. Lucarini, G. Turchetti, and S. Vaienti (2011), Numerical convergence of the block-maxima approach to the generalized extreme value distribution, *J. Stat. Phys.*, *145*, 1156–1180.

Faranda, D., G. Masato, N. Moloney, Y. Sato, F. Daviaud, B. Dubrulle, and P. Yiou (2016), The switching between zonal and blocked mid-latitude atmospheric circulation: A dynamical system perspective, *Clim. Dyn.*, *47*(5–6), 1587–1599.

Faranda D., G. Messori, and P. Yiou (2017) Dynamical proxies of North Atlantic predictability and extremes, *Sci. Rep.*, doi:10.1038/srep41278.

Ferranti, L., S. Corti, and M. Janousek (2015), Flow-dependent verification of the ECMWF ensemble over the Euro-Atlantic sector, *Q. J. R. Meteorol. Soc.*, *141*, 916–924, doi:10.1002/qj.2411.

Freitas, A. C. M., J. M. Freitas, and M. Todd (2010), Hitting time statistics and extreme value theory, *Probab. Theory Rel.*, *147*, 675–710.

Gasparrini, A., et al. (2015), Mortality risk attributable to high and low ambient temperature: A multicountry observational study, *Lancet*, *386*(9991), 369–375.

Gooding, M. J., R. H. Ellis, P. R. Shewry, and J. D. Schofield (2003), Effects of restricted water availability and increased temperature on the grain filling, drying and quality of winter wheat, *J. Cereal Sci.*, *37*(3), 295–309.

Grassberger, P. (1986), Do climatic attractors exist?, *Nature*, *323*, 609–612.

Grotjahn, R., et al. (2016), North American extreme temperature events and related large scale meteorological patterns: A review of statistical methods, dynamics, modeling, and trends, *Clim. Dyn.*, *46*(3–4), 1151–1184.

Herring, S. C., M. P. Hoerling, J. P. Kossin, T. C. Peterson, and P. A. Stott (2015), Explaining extreme events of 2014 from a climate perspective, *Bull. Am. Meteorol. Soc.*, *96*(12), S1–S172.

Johansson, Å. (2007), Prediction skill of the NAO and PNA from daily to seasonal time scales, *J. Clim.*, *20*(10), 1957–1975.

Kunkel, K. E., R. A. Pielke Jr., and S. A. Changnon (1999), Temporal fluctuations in weather and climate extremes that cause economic and human health impacts: A review, *Bull. Am. Meteorol. Soc.*, *80*(6), 1077.

Leadbetter, M. R., G. Lindgren, and H. Rootzén (1983) *Extremes and Related Properties of Random Sequences and Processes*, pp. 51–78, Springer, New York.

Lorenz, E. N. (1980), Attractor sets and quasi-geostrophic equilibrium, *J. Atmos. Sci.*, *37*, 1685–1699.
Lorenz, E. N. (1991), Dimension of weather and climate attractors, *Nature*, *353*, 241–244.
Lucarini, V., D. Faranda, and J. Wouters (2012), Universal behaviour of extreme value statistics for selected observables of dynamical systems, *J. Stat. Phys.*, *147*, 63–73.
Lucarini, V., et al. (2016), Extremes and Recurrence in dynamical systems, in *Pure and Applied Mathematics: A Wiley Series of Texts, Monographs and Tracts*, pp. 126–172, Wiley, Hoboken, N. J.
Mann, H. B., and D. R. Whitney (1947), On a test of whether one of two random variables is stochastically larger than the other, *Ann. Math. Stat.*, *18*(1), 50–60, doi:10.1214/aoms/1177730491.
Michelangeli, P. A., R. Vautard, and B. Legras (1995), Weather regimes: Recurrence and quasi stationarity, *J. Atmos. Sci.*, *52*(8), 1237–1256.
Pickands, J., III (1975), Statistical inference using extreme order statistics, *Ann. Stat.*, *3*, 119–131.
Sene, K. (2008), *Flood Warning, Forecasting and Emergency Response*, pp. 1–18, Springer Science & Business Media, Berlin.
Süveges, M. (2007), Likelihood estimation of the extremal index, *Extremes*, *10*(1–2), 41–55.
Vannitsem, S. (2001), Toward a phase-space cartography of the short and medium range predictability of weather regimes, *Tellus*, *53A*, 56–73.
Vautard, R., and M. Ghil (1989), Singular spectrum analysis in nonlinear dynamics, with applications to paleoclimatic time series, *Phys. D*, *35*, 395–424.
Yiou, P., and M. Nogaj (2004), Extreme climatic events and weather regimes over the North Atlantic: When and where?, *Geophys. Res. Lett.*, *31*, L07202, doi:10.1029/2003GL019119.